2005-01-01

Optimum Design of the Printed Strip Monopole

Max Ammann
Technological University Dublin, max.ammann@tudublin.ie

Matthias John
Technological University Dublin, matthias.john@tudublin.ie

Recommended Citation

Amman, M. & John, M. (2005) Optimum Design of the Printed Strip Monopole. *IEEE Antennas and Propagation Magazine*, December, 2005, vol.47, no. 6, pp.59-61. doi:10.1109/MAP.2005.

Optimum Design of the Printed Strip Monopole

M. J. Ammann and M. John

Centre for Telecommunications Value-Chain Driven Research, School of Electronic & Communications Engineering
Dublin Institute of Technology, Kevin St. Dublin 8, Ireland
E-mail: mammann@electronics.dit.ie

Abstract

A monopole antenna, printed on low-cost laminate and fed by a microstrip line, is examined. These types of antennas are becoming popular in view of their broad bandwidth and low-profile structure, enabling easy integration as a terminal antenna. The move away from a classical ground plane (with normal radiator) is one of the attractive features of these antennas, but the full effects of the radiator and ground plane being on opposite sides of the same laminate are often not investigated. The effect of these ground planes on the impedance bandwidth and radiation pattern is investigated experimentally and numerically.

Keywords: Microstrip antennas; monopole antennas; antenna measurements; ground plane

1. Introduction

The monopole antenna is an attractive antenna for modern communications systems, due to its simplicity, broad bandwidth, and quasi-omnidirectional radiation properties. The planar monopole has a considerably larger bandwidth, and has made the monopole more attractive for wideband wireless communications [1, 2]. However, the ground-plane size and orientation with respect to the radiator can place physical limitations on the use of such antennas. In recent years, there has been a move toward the printed-monopole type of antenna, with the ground plane printed on the same substrate, parallel to the radiator [3, 4]. This has made the antenna low in profile, low in volume, easier to fabricate, and suitable for integration into the circuit board as a terminal antenna. Many of these microstrip-fed monopole-style antennas have since been reported, such as the inverted-F antenna, and many are multi-band structures [5-7]. Multiple-element monopoles for diversity have been reported [8], and fractal techniques have been employed [9]. The dependence of these antenna types on the ground-plane dimensions is often not fully considered. This dependence can be more easily observed when a simple element, such as a strip monopole, is investigated. For this purpose, a strip monopole was fabricated symmetrically with respect to the ground plane, and fed by a straight microstrip line. In practice, the strip may not be symmetrically located, and it may be fed by a microstrip line that is partially at right angles to the strip.

2. Antenna Construction and Modeling

The monopole was printed on one side of an FR4 substrate, and the ground plane was located on the opposite side. The antenna was fed by a 50 Ω microstrip line, of width $w = 2.4$ mm. This line extended above the ground plane by a length $l = 30$ mm

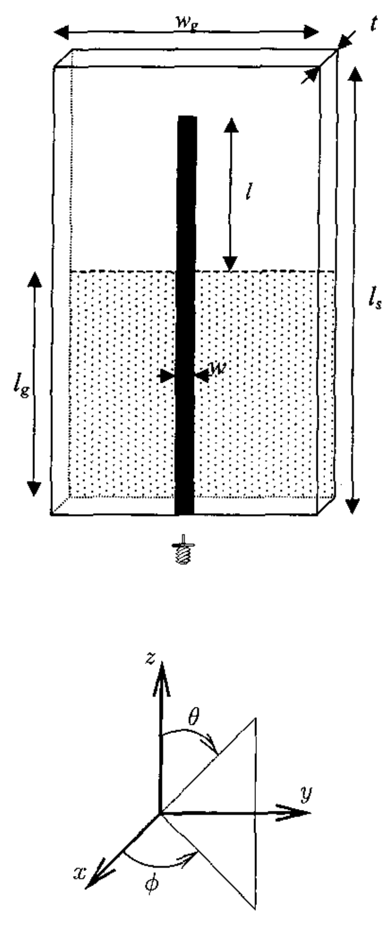

Figure 1. The geometry of the printed strip monopole, showing the coordinate system.

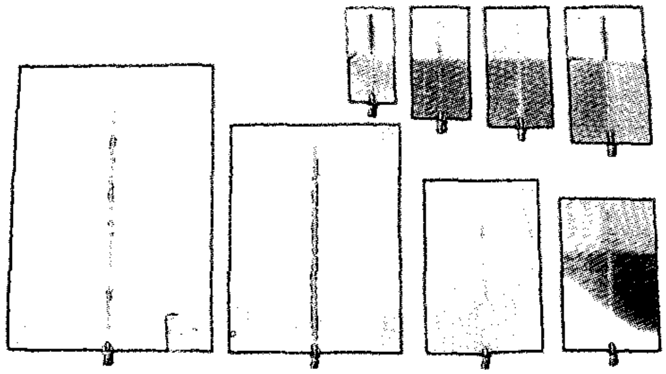

Figure 2. A photograph of the antennas with different ground-plane sizes.

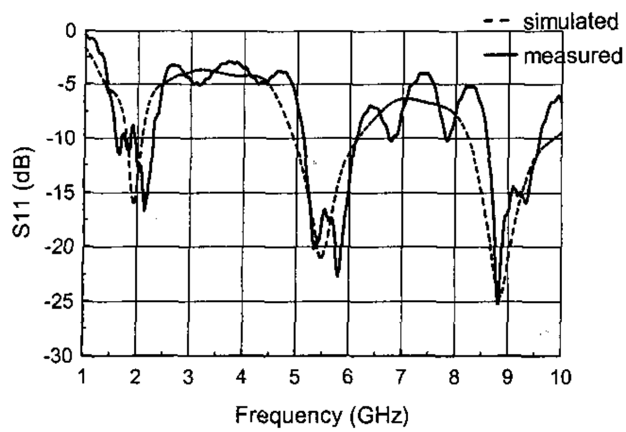

Figure 3. The measured and simulated return loss as a function of frequency for the strip monopole with a ground-plane size of 70 × 70 mm.

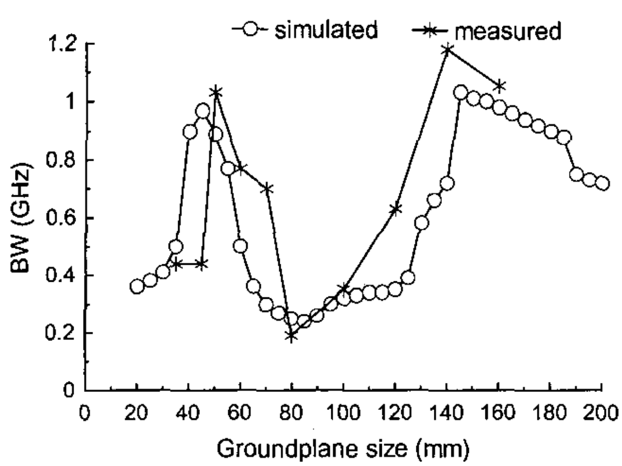

Figure 4. The measured and simulated impedance bandwidth (10 dB return loss) for the first resonance, plotted against the ground-plane size.

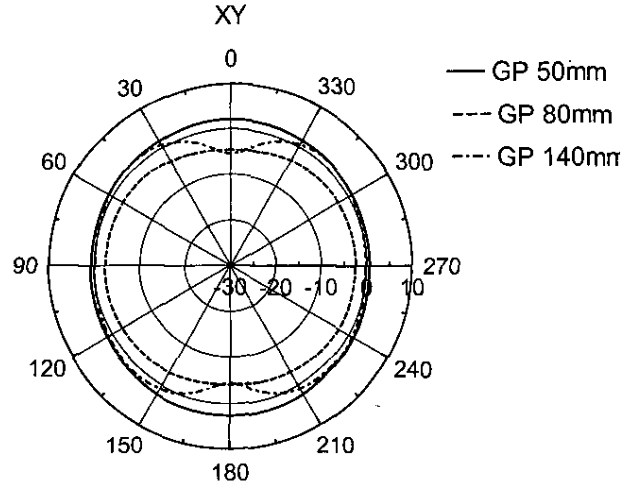

Figure 5a. The radiation patterns for the *xy* plane for ground-plane sizes of 50 × 50 mm, 80 × 80 mm, and 140 × 140 mm.

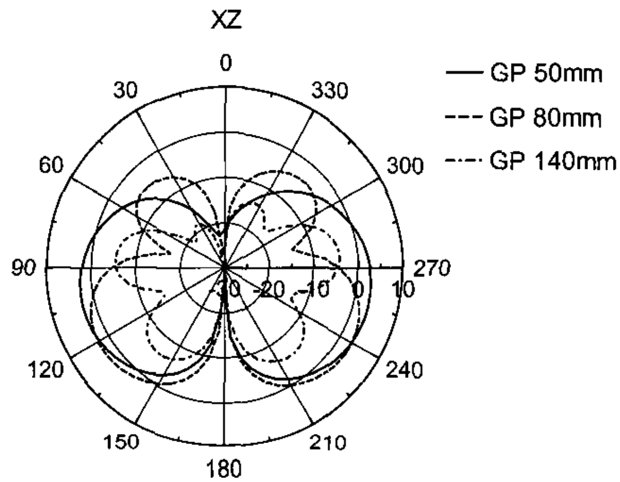

Figure 5b. The radiation patterns for the *xz* plane for ground-plane sizes of 50 × 50 mm, 80 × 80 mm, and 140 × 140 mm.

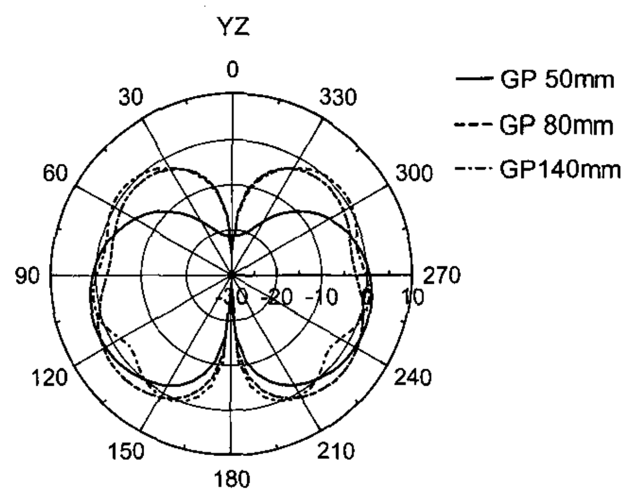

Figure 5c. The radiation patterns for the *yz* plane for ground-plane sizes of 50 × 50 mm, 80 × 80 mm, and 140 × 140 mm.

($0.2\lambda_0$ at 2 GHz). The ground plane was square, with dimensions $l_g \times w_g$, which were varied from 30 × 30 mm to 160 × 160 mm. The antenna was fed using an SMA microstrip connector. The antenna and coordinate system are shown in Figure 1. The substrate parameters were 1 oz/sq. ft. EDC, $\tan\delta = 0.02$, $\varepsilon_r = 4.3$, and $t = 1.6$ mm. For all ground-plane sizes, the substrate extended 10 mm above the monopole, i.e., $l_s = l + l_g + 10$ mm. The antennas were fabricated on a LPKF protomat milling unit. A photograph is shown in Figure 2.

The modeling technique employed was finite-integration time-domain (CST Microwave Studio), which produced good agreement with experimental data. A waveguide port was employed, and the number of mesh cells was 40,565.

3. Impedance Bandwidth

The return loss was measured on a Rohde & Schwarz ZVB vector network analyzer, and then compared with simulation for the full range of ground-plane sizes. The 10 dB-return-loss bandwidth for the first resonance was compared in each case. A plot of the measured and simulated return losses as a function of frequency for a ground plane size of 70 × 70 mm is shown in Figure 3. A comparison of simulated and measured bandwidth plotted against ground-plane size is shown in Figure 4. It can be seen that the agreement was good, and that the measured bandwidth had maximum values for ground-plane sizes of 50 mm (45 mm simulated) and 140 mm (measured and simulated). It could be observed that the bandwidth fell sharply as the ground-plane size deviates from 50 mm. This was due to the presence of ground-plane resonant modes. Hence, the ground-plane size must be chosen based on the bandwidth requirement. For the 50 × 50 mm ground plane, the measured bandwidth was 1.05 GHz, which represented a fractional impedance bandwidth of 58%.

4. Radiation Patterns

The simulated radiation efficiency for a 50 mm ground plane was found to be 93% at 2 GHz. The use of FR4 did not reduce the maximum gain by more that 0.3 dB at this frequency, compared to a low-loss microwave laminate.

The radiation patterns were simulated using CST, and are illustrated in Figure 5. The patterns are shown for ground-plane sizes of 50 mm, 80 mm, and 140 mm, representing the sizes corresponding to the maximum and minimum impedance bandwidths (see Figure 4). The H-plane ($E_\theta, \theta = 90°$) patterns were omnidirectional for the small (50 mm) ground plane, but it can be seen that the gain dropped considerably normal to the ground plane (for $\phi = 0°$ and 180°) as the ground-plane size increased. For a ground plane of 140 mm, the gain fell by about 8 dB in these directions. This was due to distortion of the image, because the image was ϕ dependent. The E-plane patterns were seen to be more dipole-like than classical monopoles above finite ground planes. The patterns for the $E_\theta, \phi = 0°$ and $E_\theta, \phi = 90°$ planes (*xz* and *yz*) are shown in Figures 5b and 5c. The generally exhibited more radiation below the ground plane than above for all ground-plane sizes. It can be seen that the maximum gain was about 3.0 dBi, which was stable with frequency (±1 dB) over the impedance bandwidth of the antenna.

5. Conclusion

It was observed that the impedance bandwidth for a printed monopole was strongly dependent on the ground-plane size. Hence, in an ideal situation, the ground-plane size should be chosen based on bandwidth requirements. The radiation pattern exhibited omnidirectional features in the H plane for smaller ground-plane sizes, with an increased loss of omnidirectionality as the ground-plane size increased. The E-plane pattern exhibited increased energy below the ground plane compared with classical ground-plane arrangements.

6. References

1. P. Agrawall, G. Kumar, and K. Ray, "Wideband Planar Monopole Antennas," *IEEE Transactions on Antennas and Propagation*, **AP-46**, 2, 1998, pp. 294-295.

2. M. J. Ammann and Z. N. Chen, "A Wideband Shorted Planar Monopole with Bevel," *IEEE Transactions on Antennas and Propagation*, **AP-51**, 4, 2003, pp. 901-903.

3. M. Ali and G. H. Hayes, "Analysis of Integrated inverted-F Antennas for Bluetooth Applications," *IEEE AP-S Conference on Antennas and Propagation for Wireless Communications*, 2000, pp. 21-24.

4. Y L Kuo, T W Chiou and K L Wong, "A Novel Dual-band Inverted-F Antenna," *Microwave Opt. Technol. Lett.*, **31**, 2001, pp. 353-355.

5. S. H. Yeh and K. L. Wong, "Integrated-F Shaped Monopole Antenna for 2.4/5.2 GHz Dual Band Operation," *Microwave Opt. Technol. Lett.*, **34**, 1, 2002, pp. 24-26.

6. M. J. Ammann and R. Farrell, "Dual-Band Monopole Antenna with Stagger-Tuned Arms for Broadbanding," *IEEE International Workshop on Antenna Technology: Small Antennas and Novel Metamaterials*, 2005, pp. 278-281.

7. H. C. Go and Y.W. Jung, "Multi-band Modified Fork-shaped Microstrip Monopole Antenna with Ground Plane Including Dual-Triangle Portion," *Electronic Lett.*, **40**, 10, 2004, pp. 575-577.

8. Y. L. Kuo and K. L. Wong, "Dual Polarized Monopole Antenna for Wireless LAN Operation," IEEE International Symposium on Antennas and Propagation *Digest*, **4**, 2002, pp. 80-83.

9. G. Tsachtiris, C. Soras, M. Karaboikis and V. Maklos, "A Printed Folded Koch Monopole Antenna for Wireless Devices," *Microwave Opt. Technol. Lett.*, **40**, 5, 2004, pp. 374-378.